POLITECNICO DI TORINO
Repository ISTITUZIONALE

Automatic Nonlinear Subspace Identification Using Clustering Judgment Based on Similarity Filtering

Original
Automatic Nonlinear Subspace Identification Using Clustering Judgment Based on Similarity Filtering / Zhu, R., Jiang, D., Marchesiello, S., Anastasio, D., Zhang, D., Fei, Q.. - In: AIAA JOURNAL. - ISSN 1533-385X. - ELETTRONICO. - (2023), pp. 1-9. [10.2514/1.J062816]

Availability:
This version is available at: 11583/2976412 since: 2023-03-08T10:20:08Z

Publisher:
American Institute of Aeronautics and Astronautics

Published
DOI:10.2514/1.J062816

Terms of use:

This article is made available under terms and conditions as specified in the corresponding bibliographic description in the repository

Publisher copyright
AIAA preprint/submitted version e/o postprint/Author's Accepted Manuscript

(Article begins on next page)

10 September 2026

Politecnico di Torino

Automatic nonlinear subspace identification using clustering judgment based on similarity filtering

Rui Zhu,
Southeast University, Nanjing, Jiangsu Province, 210000, China;
Technical University of Munich, Munich, Bavaria, 80333, Germany;

Dong Jiang,
Nanjing Forestry University, Nanjing, Jiangsu Province, 210000, China

Stefano Marchesiello, and Dario Anastasio
Politecnico di Torino, Torino, 10121, Italy

Dahai zhang , and Qingguo Fei
Southeast University, Nanjing, Jiangsu Province, 210000, China

https://doi.org/10.2514/1.J062816

Cite as:

R. Zhu, D. Jiang, S. Marchesiello, D. Anastasio, D. Zhang, Q. Fei, Automatic Nonlinear Subspace Identification Using Clustering Judgment Based on Similarity Filtering, AIAA Journal 0 0:0, 1-9. doi: 10.2514/1.J062816

Automatic nonlinear subspace identification using clustering judgment based on similarity filtering

Rui Zhu [1],
Southeast University, Nanjing, Jiangsu Province, 210000, China;
Technical University of Munich, Munich, Bavaria, 80333, Germany;
Dong Jiang [2],
Nanjing Forestry University, Nanjing, Jiangsu Province, 210000, China
Stefano Marchesiello [3], and Dario Anastasio [4]
Politecnico di Torino, Torino, 10121, Italy
Dahai zhang [5], and Qingguo Fei [6]
Southeast University, Nanjing, Jiangsu Province, 210000, China

Accurately determining the system order plays a vital role in system identification directly related to the accuracy of identification results, especially for nonlinear system identification. Due to the need for human subjective judgment, the traditional sequence determination method easily causes uncertainty in the results, and the phenomenon of virtual mode or omission occurs. An automatic nonlinear subspace identification method is proposed to address the above problems. When the eigenvalue decomposition of the constructed Hankel matrix is performed, the calculation range of the modal order of the system is estimated. The similarity coefficient and distance function are introduced to cluster the identified modal results, the poles of the false modes are removed to obtain the cluster stabilization diagram, and the best order of the system is received. Then the modal parameters and nonlinear coefficients are obtained. Simulation examples are carried out to verify the effectiveness and robustness of the proposed method. An experimental study is carried out on a multilayer building with nonlinear characteristics. Compared with the traditional stabilization graph, the accuracy of the automatic order determination proposed in this paper is proved.

---

[1] Postdoc researcher, Institute of Flight System Dynamics, r.zhu@tum.de

[2] Associate professor, School of Mechanical and Electronic Engineering, jiangdong@njfu.edu.cn.

[3] Professor, Dipartimento di Ingegneria Meccanica ed Aerospaziale, stefano.marchesiello@polito.it

[4] Research fellow, Dipartimento di Ingegneria Meccanica ed Aerospaziale, dario.anastasio@polito.it

[5]Associate professor, School of Mechanical Engineering, Corresponding author, dzhang@seu.edu.cn.

[6] Professor, School of Mechanical Engineering, Corresponding author, qgfei@seu.edu.cn.

Nomenclature

(Nomenclature entries should have the units identified)

$\boldsymbol{A}$ = dynamical system matrix of the state-space model

$\boldsymbol{A}_c$ = dynamical system matrix of the continuous-time state-space model

$\boldsymbol{B}$ = input matrix

$\boldsymbol{B}_c$ = input matrix of the continuous-time state-space model

$\boldsymbol{C}$ = output matrix

c = damping

$\boldsymbol{C}_d$ = viscous damping matrix

$\boldsymbol{D}$ = direct feedthrough matrix of the state-space model

$f(t)$= force vector

$\boldsymbol{H}$ = underlying linear system receptance matrix

$\boldsymbol{H}_E$= "extended" frequency response function (FRF) matrix

$\boldsymbol{K}$ = stiffness matrix

k = stiffness

$\boldsymbol{M}$ = mass matrix

m = mass

NSI= nonlinear subspace identification

p = eigenvalue of the system matrix

r = natural frequency

x = state vector

z = displacement vector

ω = angular frequency

ξ = damping ratio

α = coefficient of nonlinear damping

Δt = sampling period

I. Introduction

In engineering, system identification [1][2] plays a significant role, which can provide theoretical support for response analysis [3], fault diagnosis, safety evaluation, and structural optimization [4]. This process can be applied to linear systems [5] and nonlinear ones [6][7]. Regardless of the type of system, determining the best model order is directly related to the accuracy of the identification result.

In general, Singular Value Decomposition is used to evaluate system order in the linear methods. The order of the system is determined by examining the difference between two adjacent singular values, where the number of singular values before the maximum difference is the order of the system. However, the higher-order singular values of the matrix are not zero in real systems due to noise, often causing modal omission and spurious modal phenomena [8][9]. Different techniques were introduced to reduce user interaction. Vanlanduit et al. [10] proposed an automatic modal parameter estimation algorithm based on the maximum likelihood estimator. By making use of a clustering algorithm, the classification of physical and computational poles could be performed in an automatic manner. Zhang et al. [11] introduced the component energy index to measure the energy contribution of signal components. In this way, the order estimate is given in terms of component energy index rather than matrix singular values to avoid underestimating the state space model order. A new covariance driven stochastic subspace identification method [12] based on the automatic analysis of stabilization diagrams is proposed, successfully identifying a long-span arch bridge first 12 modes. Ni et al. [13] apply a recursive algorithm without SVD to determine the time-varying modal parameters. For the continuous real-time monitoring of structures, Bakir [14] proposed the Modal Phase Collinearity index to eliminate false modal poles and then used hierarchical clustering to perform large-scale clustering of real modalities. Rainieri et al. [15] developed an automated output-only modal parameter estimation, set the element count threshold as a function of the size of the hierarchical clustering dendrogram, and obtained candidate modalities for the true modalities. To sum up, in view of the problem of underestimating or overestimating the model order, scholars have conducted much research on linear structures and less on the problem of order determination of nonlinear structures. Nonlinear subspace identification (NSI) has been extensively developed recently[16][17][18]. Zhu et al. [19] broadened the method to recognize nonlinear damping and combined Bayesian methods [20] to discuss unknown models. Noël et al. [21] first introduce the stabilization diagrams in the presence of nonlinearity, and the results show the proposed method is effective for retrieving linear system parameters from nonlinear data. Marchesiello et al. [22] investigated the impact of spurious poles on the

nonlinear subspace identification and introduced some modal decoupling tools, finally identifying the modal contributions of physical poles on the nonlinear dynamics.

This paper proposes an automatic nonlinear system identification method using clustering judgment based on similarity filtering. Based on the traditional stabilization graph in NSI, a modal matrix and a distance function are constructed. Through clustering judgment based on similarity distance for each order mode, the number of modes that reach a predetermined scale is taken as the best order of the structure to avoid human judgment errors. The rest of this paper outline is as follows: Section II. A introduces the characterization of nonlinearity. Section II.B obtains the underlying frequency response function based on NSI. Automatic determination of modal order based on the Jaccard similarity coefficient is presented in Section II.C. Section III investigates the numerical simulation of the MDOF system with cubic stiffness and Coulomb friction. Section IV presents an experimental study on multilayer building with nonlinearity. The conclusions are drawn in Sect. V.

II. Theory

As known, nonlinear subspace identification [19] establishes the relationship between the underlying frequency response function and the nonlinear parameters. The accuracy of the nonlinear subspace identification method mainly depends on two factors, one is the nonlinear characterization, and the other is the order determination of the underlying linear system. The former has been studied in previous work [19], and the latter is the focus of this work.

The equation of motion of a nonlinear system with r nonlinear parameters (nonlinear springs or dampers) can be described as

$$\boldsymbol{M}\ddot{z}(t)+\boldsymbol{C}\dot{z}(t)+\boldsymbol{K}z(t)+\sum_{i=1}^{r}\lambda_i l_i W_i\left(z,\dot{z},t\right)=f(t) \tag{1}$$

where $\boldsymbol{M}\in R^{n\times n}$, $\boldsymbol{C}\in R^{n\times n}$, and $\boldsymbol{K}\in R^{n\times n}$ are the mass, viscous damping, stiffness matrices, $z(t)$ is the generalized displacement vector, and $f(t)$ is the force vector. The nonlinear term is expressed as the sum of r components, each depending on the nonlinear scalar function $W_i(t)$ through a vector l_i, which indicates the nonlinear element's location and whose entries may assume the values 1, -1, or 0. λ is the identified nonlinear coefficient in Fig. 1.

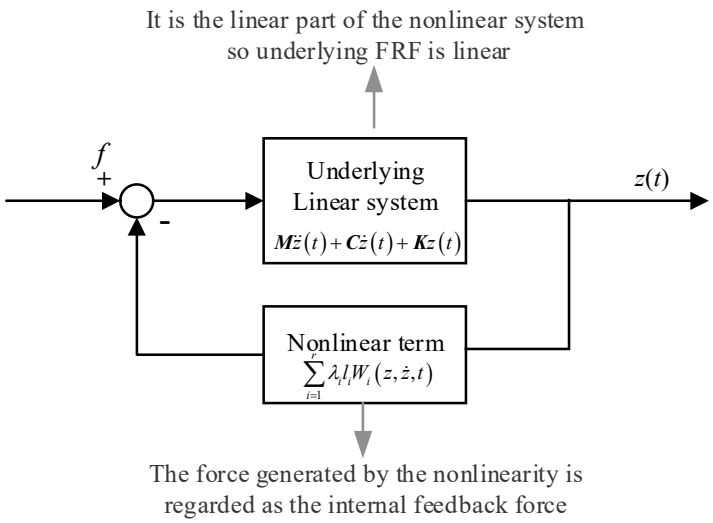

Fig. 1 Closed-loop representation with nolinearity

A. Characterization of nonlinearity

The classical way of applying the nonlinear subspace identification techniques requires a characterization step, which defines the nonlinear basis functions $G_i(t)$ and the location of the nonlinearities. Typically, the restoring force surface method (RFS) can be used to have an initial guess about the nonlinear functions to include in the subspace analysis. The RFS constructs the three-dimensional point set between restoring internal force, velocity, and displacement.

Eq. (1) can be rewritten as

$$\boldsymbol{M}\ddot{z}(t)+F(z,\dot{z})=f(t) \tag{2}$$

where $F(x,\dot{x})$ is restoring force of the system, and it can be expressed as

$$F(z,\dot{z})=\boldsymbol{C}\dot{z}(t)+\boldsymbol{K}z(t)+\sum_{i=1}^{r}\lambda_i W_i(z,\dot{z},t)=f(t)-\boldsymbol{M}\ddot{z}(t) \tag{3}$$

The intersection line between the surface with displacement x=0 and the restoring force surface can be obtained in [19]. This line represents the relationship between speed and restoring force, and represents the characteristics of system damping. More recently, a Bayesian approach has been developed to better characterize the nonlinear functions included in NSI [20].

B. Underlying Frequency Response Function

The equation of motion of a nonlinear system can be expressed as the state-space formulation. The state vector is chosen as $x=\begin{bmatrix} z & \dot{z} \end{bmatrix}^T$, the state-space formulation is described as

$$\begin{Bmatrix} \dot{z} \\ \ddot{z} \end{Bmatrix} = \underbrace{\begin{bmatrix} 0 & I \\ -M^{-1}K & -M^{-1}C \end{bmatrix}}_{A_c} \begin{Bmatrix} z \\ \dot{z} \end{Bmatrix} + \underbrace{\begin{bmatrix} 0 & 0 & \cdots & 0 \\ M^{-1}\lambda_1 l_1 & M^{-1}\lambda_2 l_2 & \cdots & M^{-1}\lambda_r l_r \end{bmatrix}}_{B_c} \begin{Bmatrix} f(t) \\ -W_1(t) \\ \vdots \\ -W_r(t) \end{Bmatrix} \tag{4}$$

$$y = \underbrace{\begin{bmatrix} I_{n\times n} & 0_{n\times n} \end{bmatrix}}_{C} \begin{Bmatrix} z \\ \dot{z} \end{Bmatrix} + \underbrace{0_{n\times n} \quad 0_{n\times 1} \quad \cdots \quad 0_{n\times 1}}_{D} \begin{Bmatrix} f(t) \\ -W_1(t) \\ \vdots \\ -W_r(t) \end{Bmatrix} \tag{5}$$

where $\boldsymbol{A}_c$ is the dynamical system matrix of the continuous-time state-space model, $\boldsymbol{B}_c$ is the input matrix of the continuous-time state-space model, $\boldsymbol{C}$ is the output matrix, and $\boldsymbol{D}$ is the direct feedthrough matrix of the state-space model.

Meanwhile, the dynamical system matrix of the discrete state-space model $\boldsymbol{A}$ can be obtained

$$\boldsymbol{A} = e^{\boldsymbol{A}_c \Delta t} \tag{6}$$

where Δt is the sampling period.

The input matrix $\boldsymbol{B}$ is

$$\boldsymbol{B} = \left(e^{\boldsymbol{A}_c \Delta t} - I_{2h\times 2h} \right) \boldsymbol{A}_c^{-1} \boldsymbol{B}_c \tag{7}$$

The nonlinear subspace identification procedure is based on estimating the state space matrices $\boldsymbol{A}$, $\boldsymbol{B}$, $\boldsymbol{C}$, and $\boldsymbol{D}$ obtained within a similarity transformation. Due to the nonlinear parameters, the "extended" frequency response function (FRF) matrix is expressed as

$$\boldsymbol{H}_E(\omega) = \boldsymbol{D} + \boldsymbol{C}\left(z\boldsymbol{I}_{2h\times 2h} e^{\boldsymbol{A}_c \Delta t} - \boldsymbol{A} \right)^{-1} \boldsymbol{B}, z = e^{i\omega\Delta t} \tag{8}$$

After some mathematical manipulations [16], it can be proven that

$$\boldsymbol{H}_E(\omega) = \begin{bmatrix} \boldsymbol{H} & \boldsymbol{H}\lambda_1 l_1 & \cdots & \boldsymbol{H}\lambda_r l_r \end{bmatrix} \tag{9}$$

where

$$\boldsymbol{H}(\omega) = \left(\boldsymbol{K} + i\omega\boldsymbol{C}_d - \omega^2 \boldsymbol{M} \right)^{-1} \tag{10}$$

is the underlying linear system receptance matrix. The nonlinear coefficients λ_i can be identified in Eq.(9), which are complex-valued and frequency-dependent. Ideally, the real parts of the coefficients converge to their exact values, independent of frequency, while the imaginary parts are relatively small [16].

General, the model order n can be confirmed as the singular value decomposition. As mentioned in Ref.[20], the singular value decomposition (SVD) of the following weighted oblique projection is performed:

$$\vartheta_i \Pi_{W_f^+}^{\perp} = \bar{U} S V^T = \begin{bmatrix} \bar{U}_1 & \bar{U}_2 \end{bmatrix} \begin{bmatrix} S_1 & 0 \\ 0 & S_2 \end{bmatrix} \begin{bmatrix} V_1^T \\ V_2^T \end{bmatrix} \tag{11}$$

where S_1 can be expressed：

$$S = \begin{pmatrix} S_1 & 0 \\ 0 & S_2 = 0 \end{pmatrix}; S_1 = \mathrm{diag}\left[\sigma_i\right]; \sigma_1 \geq \sigma_2 \geq \mathrm{L} \geq \sigma_n \geq 0 \tag{12}$$

where the number of non-zero elements is the order of the underlying linear system.

When the matrix A can be estimated, the eigenvalue decomposition is implemented

$$\boldsymbol{A} = \boldsymbol{\Psi \Lambda \Psi^{-1}} \tag{13}$$

Where $\boldsymbol{\Lambda} = diag\left[\mu_i\right]$ represents a diagonal matrix of eigenvalues， $\boldsymbol{\Psi}$ represents a matrix of eigenvectors.

$$p_i = \frac{\ln \mu_i}{\Delta t} \tag{14}$$

where p_i represents the eigenvalues of the system matrix; Δt is the minimum sampling time.

Thus, the natural frequency and damping ratio are obtained:

$$p_i, \bar{p}_i = -\xi_i r_i \pm j r_i \sqrt{1-\xi_i^2} \tag{15}$$

The *i-th* order natural frequency r_i, damping ratio ξ_i and mode shape $\boldsymbol{\Phi}_i$ are:

$$r_i = \sqrt{|\, p_i \,|} \tag{16}$$

$$\xi_i = -\frac{p_i + \bar{p}_i}{2\sqrt{p_i \bar{p}_i}} \tag{17}$$

$$\boldsymbol{\Phi}_i = \boldsymbol{C \Psi}_i \tag{18}$$

C. Automatic determination of modal order based on Jaccard similarity coefficient

First of all, it is necessary to determine the minimum order and maximum order, and the real order of the system needs to be included in this range. The initial calculation order of the system is 2, and the maximum order is

determined according to eigenvalue decomposition based on Eq. (12). Taking the value that accounts for 90% of the eigenvalues as the assumed true order $\tilde{n}$, the maximum calculation order is $10\tilde{n}$, then the modal order is $10\tilde{n}$ /2=$5\tilde{n}$ because the modal order is 1/2 of the system order.

When the calculation order range is determined, the nonlinear subspace algorithm is used to identify the modal parameters of the potential linear system of the structure, and $5\tilde{n}$ groups of identification results are obtained, including the frequency values and the damping ratios.

The $5\tilde{n}$ group recognition result is regarded as a $5\tilde{n}$ class, a $5\tilde{n}$ subset is established, and the $5\tilde{n}$ subset is written into the lower triangular matrix $\boldsymbol{G}$. The distance function is used to judge the similarity of frequency and damping ratio, and the modal square matrix is constructed as follows:

$$\boldsymbol{G}=\begin{Bmatrix} (r_1,d_1)^1 & 0 & 0 & \mathrm{L} & 0 \\ (r_1,d_1)^2 & (r_2,d_2)^2 & 0 & \mathrm{L} & 0 \\ (r_1,d_1)^3 & (r_2,d_2)^3 & (r_3,d_3)^3 & \mathrm{L} & 0 \\ \mathrm{L} & \mathrm{L} & \mathrm{L} & \mathrm{O} & \mathrm{M} \\ (r_1,d_1)^{5n} & \mathrm{L} & \mathrm{L} & \mathrm{L} & (r_{5n},d_{5n})^{5n} \end{Bmatrix} \tag{19}$$

where $g_j^i=(r_j,d_j)^i$ represents j^{th} element in i^{th} group, r_j is the j^{th} modal frequency and d_j is the j^{th} modal damping.

Jaccard similarity coefficient [23] is a statistic used to compare the similarity and diversity of sample sets. The Jaccard coefficient can measure the similarity of a finite sample set, which is defined as the ratio between the size of the intersection and the size of the union of two sets

$$J(U,V)=\frac{|U\cap V|}{|U\cup V|}=\frac{|U\cap V|}{|U|+|V|-|U\cap V|} \tag{20}$$

If U and V are coincident, then define $J(U, V) = 1$. So there is

$$0\le J(U,V)\le 1 \tag{21}$$

The i-th column modal vector $(r_i, d_i)^a$ in the parameter result of group a and the modal vector $(r_j, d_j)^b$ of the j-th column in the parameter result of group b are regarded as two sets, and the similarity of the two sets is computed:

$$J\left(g_i^a,g_j^b\right)=\frac{|\,g_i^a\,\mathrm{gg}_j^b\,|}{(g_i^a)^2+(g_j^b)^2-|\,g_i^a\,\mathrm{gg}_j^b\,|} \tag{22}$$

Starting from the initial set, calculate the distance between the i^{th} subset and the j^{th} subset of Jaccard in turn. To establish the distance matrix, the similarity between the vector g_i^a and the vector g_j^b needs to be considered, and the distance is defined as

$$d_J\left(g_i^a, g_j^b\right) = 1 - \frac{|\, g_i^a \, \mathrm{gg}_j^b \,|}{(g_i^a)^2 + (g_j^b)^2 - |\, g_i^a \, \mathrm{gg}_j^b \,|} \le \delta \tag{23}$$

δ is the threshold value. When d_J is set to be less than δ, the two-order modes meet the requirements of the distance function and are clustered into one class. Based on experience, the value of δ is set to =0.01. It can be adjusted according to the test noise and other factors in practical applications. When all orders are clustered, the number of modalities in each classification is counted. Since the number of data groups is $5\tilde{n}$, when the number is greater than $0.7\times5\tilde{n}$ =$3.5\tilde{n}$, the cluster is considered to be a true modal cluster. Clusters with a number less than $3.5\tilde{n}$ were regarded as false modal clusters. After clustering, the modal clustering matrix of the stable poles is obtained, and they are drawn into a cluster stabilization diagram. The number of stable axes $\check{n}$ is counted as the best order of the system, which is substituted into Eqs. (8) ~ (10) in the nonlinear subspace method. Then, modal parameters of the underlying linear FRF and nonlinear parameters can be obtained. The framework of this method is shown in Fig. 2.

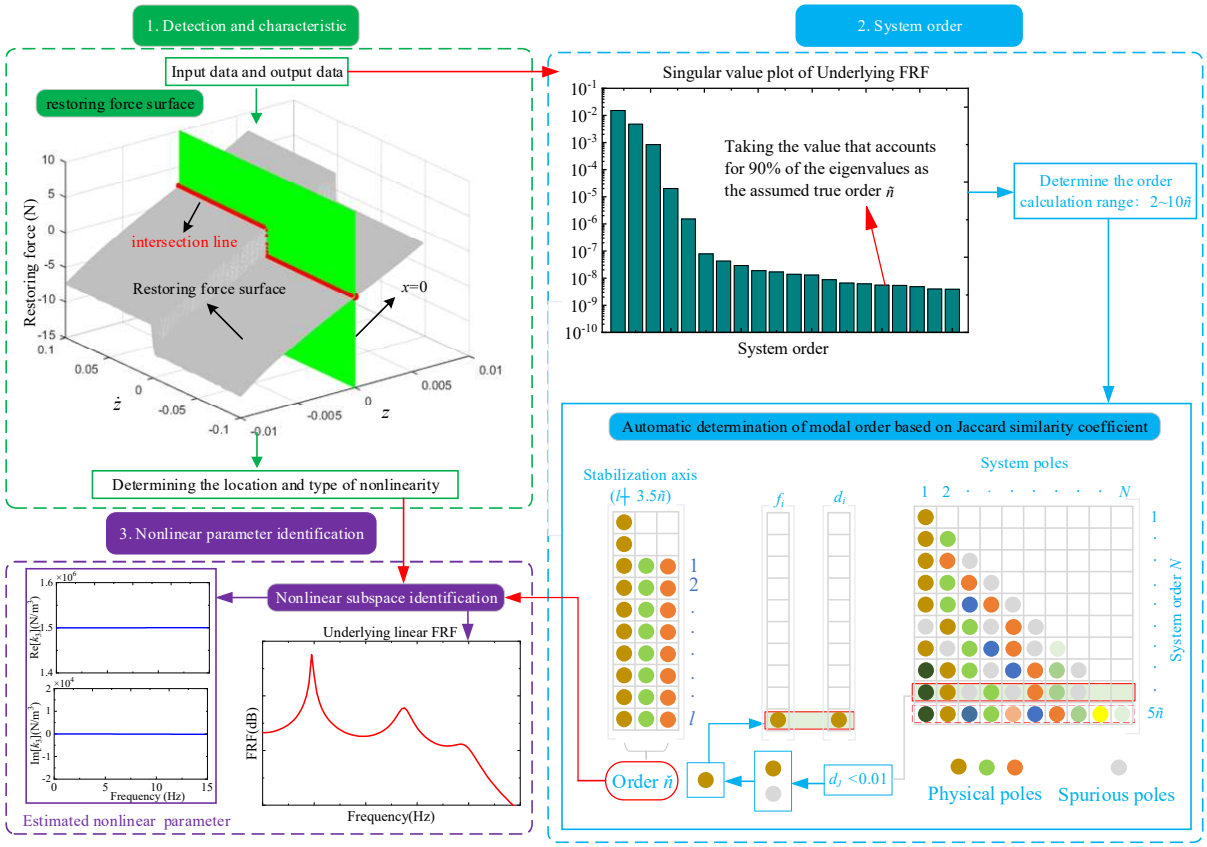

Fig. 2 Automated nonlinear subspace identification process

III. Numerical example

A numerical example is considered to demonstrate the performance of the automatic nonlinear identification approach with simulated data from MDOF systems with typical nonlinear characteristics. Consider the MDOF system with cubic stiffness and Coulomb friction depicted in Fig. 3.

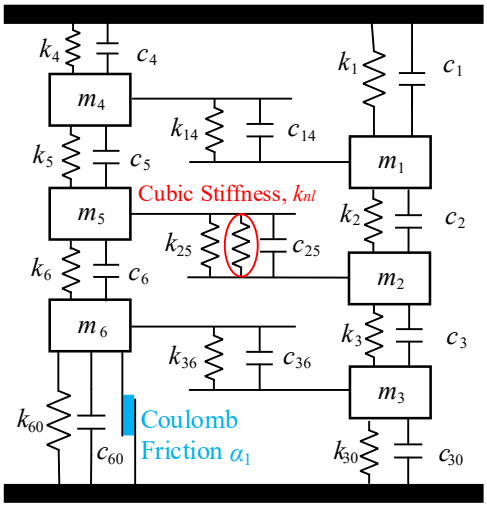

Fig. 3 A six degrees of freedom mass-spring system with cubic stiffness and Coulomb friction

The system parameters is summarized in Table 1. The type and the location of the nonlinearity can be obtained. In this section, the mode order is mainly investigated.

Table 1 System parameters of six degrees of freedom with cubic stiffness and Coulomb friction

Mass (kg)	Linear stiffness (N/m)	Damping (Ns/m)	Nonlinear stiffness	Nonlinear damping
m_1=m_3=m_5=1	k_1= k_4=6000	c_i=0.2 (i=1,2,3,4,5,6)	k_{nl} =1×10^8 N/m^3	α_1=1
m_2=m_4=m_6=0.5	k_2= k_3=2000	c_{14}= c_{25}= c_{36}=0.1		
	k_5=4000 k_6=5000	c_{30}= c_{60} =0.05		
	k_{14}= k_{25}= k_{36}=1000			
	k_{30}= k_{60} =1000			

A zero-mean Gaussian random force is selected to be applied at DOF 1, whose root-mean-square value is 30 N. Numerical integration of the equation of motion has been performed, and a total number of 10^5 samples have been generated. 2% noise of the signal standard deviation is added to the signal. The traditional stabilization diagram can be shown in Fig. 4. There are false modes, unstable poles, and stable poles for the underlying linear FRF of the nonlinear system, making it difficult to determine the order of the system.

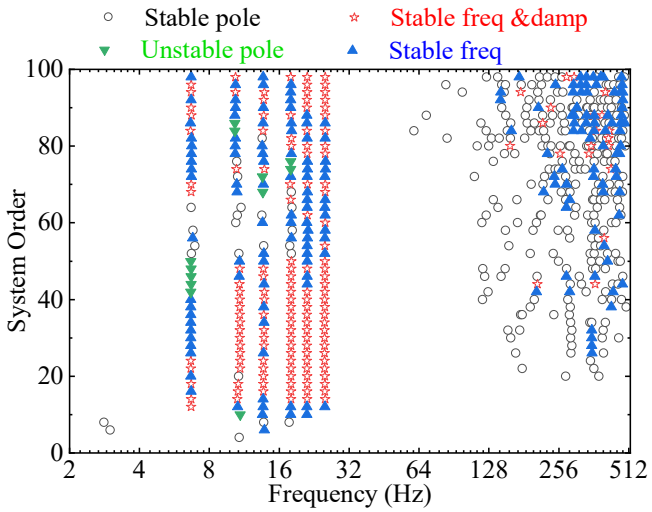

Fig. 4 The traditional stabilization diagram

Meanwhile, the proposed **c**luster stabilization diagram is described in Fig. 5 with model orders from 2~100. The similarity coefficient and distance function are used to cluster the identified modal results, the poles of the false modes are removed to obtain the cluster stabilization diagram, and the true order (n=6) of the system is obtained automatically, avoiding the influence of human judgment. The underlying estimated FRF h_{61} can be obtained as shown in Fig. 6, which is in good agreement with the true value. The modal frequencies are shown in Table 2, and the maximum error is only 2.04%.

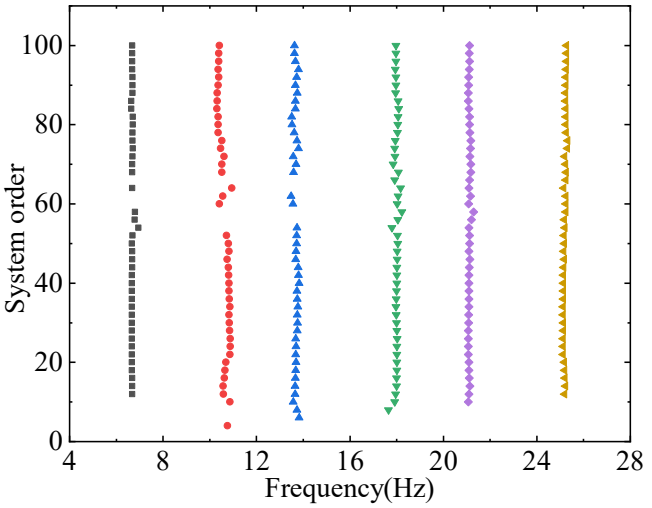

Fig. 5 The cluster stabilization diagram with the threshold value δ =0.01

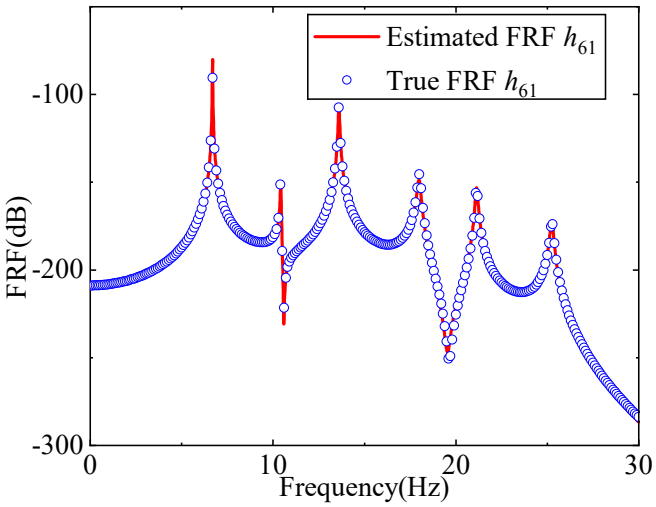

Fig. 6 Underlying FRF h_{61}

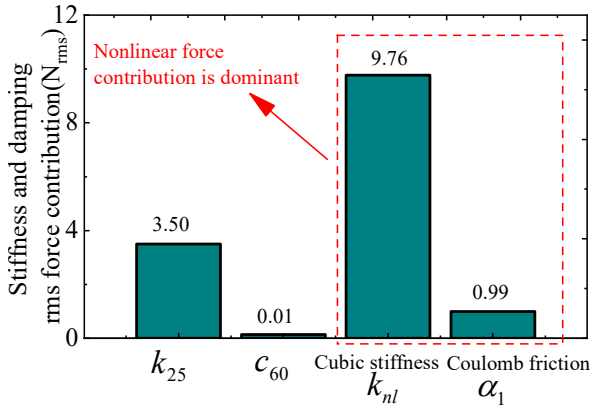

Fig. 7 Stiffness and damping rms force contributions

Table 2 Modal frequencies of underlying FRF with 2% noise

Mode order	1	2	3	4	5	6
Exact value	6.68	10.41	13.61	18.01	21.14	25.26
Identified value	6.69	10.62	13.69	18.00	21.11	25.19
Error/%	0.06	2.04	0.62	-0.08	-0.14	-0.27

The coefficients of the nonlinear basis functions can be calculated by Eq. (9) with model order n=12. Fig. 8~Fig. 9 illustrate the identified nonlinear stiffness k_3 and damping α: the frequency correlation is little, and the imaginary part is zero relative to the real part, confirming the identification quality. The nonlinear force contribution index [19] is used to evaluate the strength of nonlinearity as follows:

$$Con_{rms} = \lambda_i \times rms\left(W_i\left(z, \dot{z}\right)\right) \tag{24}$$

Force contribution is shown in Fig. 7, which show the structure has obvious cubic nonlinearity and Coulomb friction. The identified coefficients are listed in Table 3. The maximum error of the nonlinear stiffness is 4.75%,

which assesses the goodness of identification. Results show that the proposed automatic nonlinear subspace method not only effectively distinguishes the real modes from the false modes but also judges the stable axis quickly based on automated ordered cluster analysis, which verifies the validity of the method.

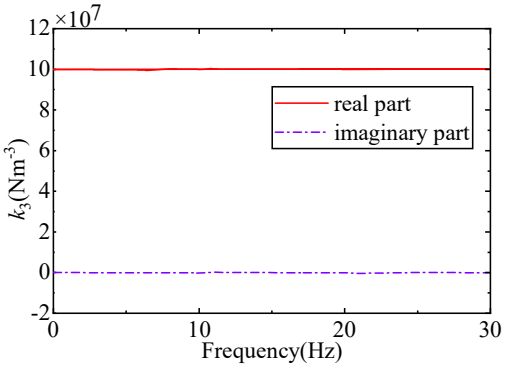

Fig. 8 Real and imaginary parts of the coefficient k_3.

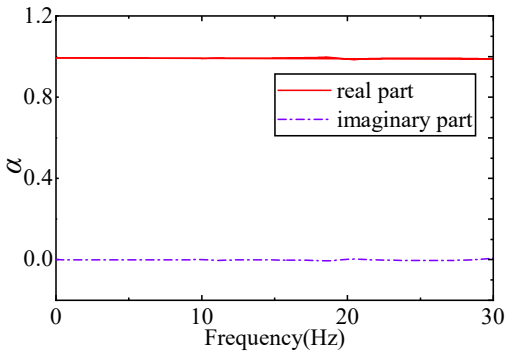

Fig. 9 Real and imaginary parts of the coefficient α.

Table 3 System parameters with noise

	Nonlinear stiffness k_3 (N/m^3)	Nonlinear damping α
Exact value	1.00×10^8	1.00
Identified value	1.03×10^8	1.0475
Error/%	3.12%	4.75%

IV. Experimental study

The multilayer building with nonlinearity is depicted in Fig. 10. The structure has been studied in [10] and [25] and the specific geometric parameters can be found in [10]. A thin wire with a small pretension is attached to the fifth layer, which makes the restoring force nonlinear if its motion is large enough. Ref. [26] indicated that the wire produces a nonlinear force of the form $f_n=k_t x_5+k_n x_5^3$. An external random is applied by using an electrodynamic shaker at the second layer of the structure, whose RMS value is 20.89 N. An acceleration sensor is arranged in each

layer, and the displacement signal can be obtained by quadratic integration of the acceleration response. The excitation and the response of the second layer are shown in Fig. 12.

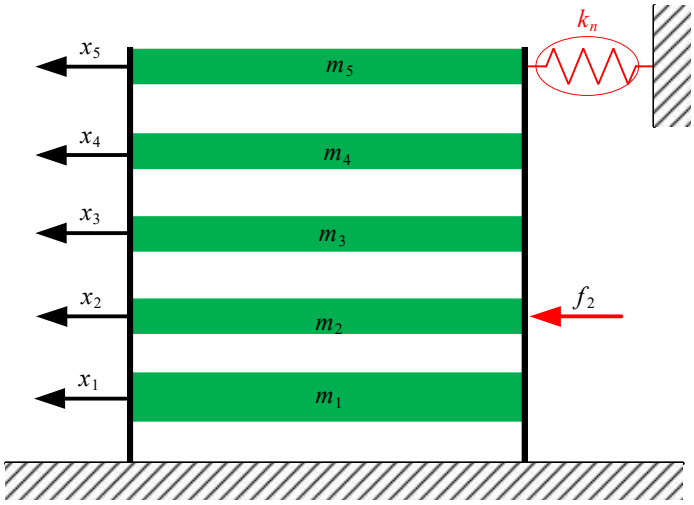

Fig. 10 The schematic of a multilayer building with nonlinearity

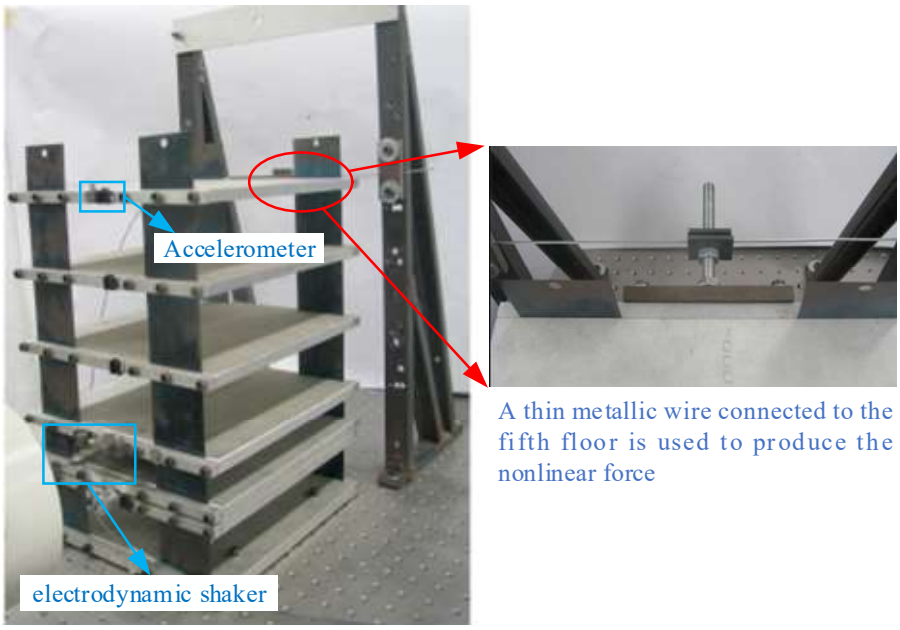

Fig. 11 The experimental photo of the multilayer building with nonlinearity

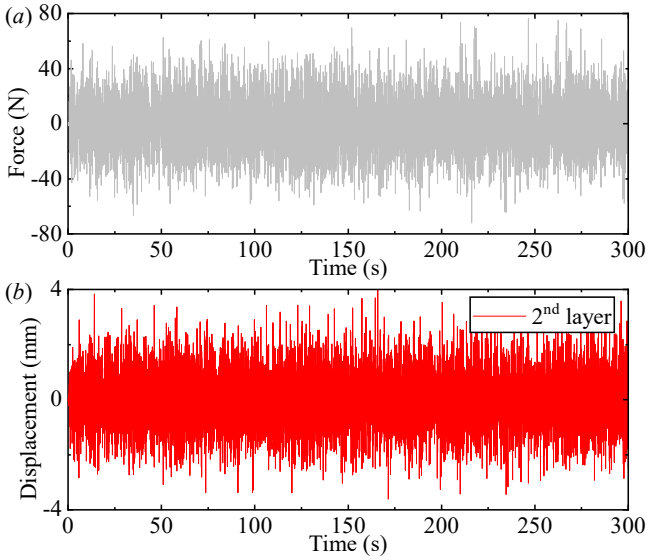

Fig. 12 Experimental test. (a) Excitation signal; (b) Time history of the second layer's displacement by quadratic integration

A first experimental characterization is carried out to check if the structure behaves nonlinearly for the selected excitation level (20.89 Nrms). To this end, a second test is performed applying a random excitation at a much lower level (0.76 Nrms). The experimental FRF h_{52} is computed in both cases using the average $H1$, $H2$ estimator, and the result is depicted in Fig. 13.

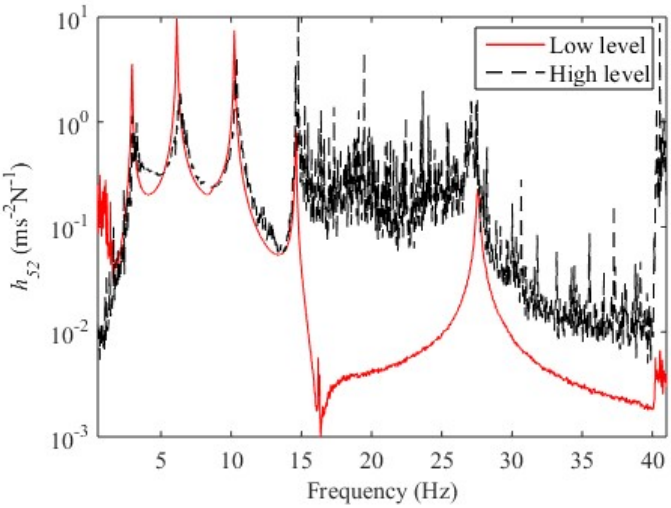

Fig. 13 Comparison between linear estimates of h_{52} at low (0.76 Nrms, red solid line) and high (20.95 Nrms, black dotted line) excitation level.

Clear signs of nonlinearity can be observed in the FRFs, mainly consisting of frequency shifts and augmented distortions. Considering now the high level case, the proposed method can be applied to estimate the parameters of

the nonlinear model.The traditional stabilization diagram can be shown in **Fig. 14**; there are false modes, unstable poles, and stable poles. For comparison, the proposed **c**luster stabilization diagram is described in **Fig. 15**. There are five groups of clusters, so the modal order of the system is n=5, and the proposed method can effectively avoid false modes. Then, the modal frequency of each order can be obtained by averaging each group of cluster identification results. The coefficient of the nonlinear basis functions can be calculated by Eq. (9) with model order n=10. The real part and imaginary part of the nonlinear coefficient can be shown in **Fig. 16** between 2 and 15 Hz. A spectral mean in this range is a reasonable choice because the real part is higher than the imaginary part, with a real/imaginary ratio of roughly 36. The real part also shows a stable behavior, confirming the quality of the estimation. The mean value of the real part is k_n= 6.11×10^7 N/m^3, with a standard deviation of 1.78×10^4 N/m^3. This result is consistent with the one in [10], which was 6.28×10^7 N/m^3.

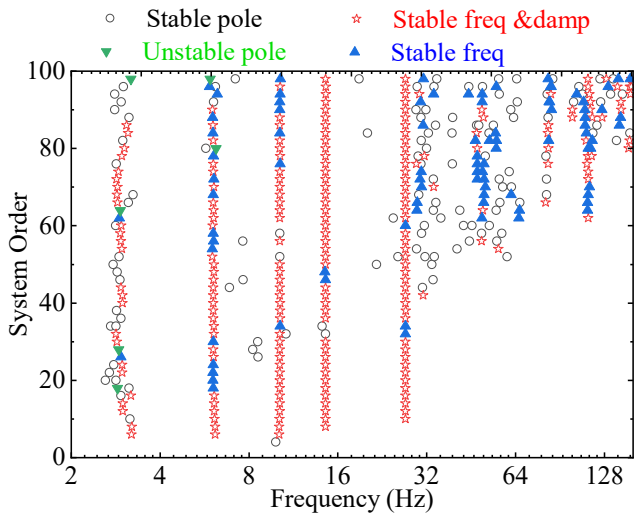

Fig. 14 The traditional stabilization diagram

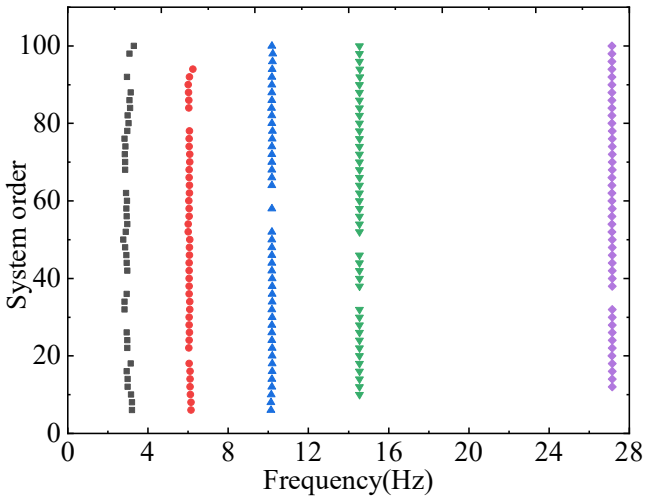

Fig. 15 The cluster stabilization diagram with the threshold value δ =0.01

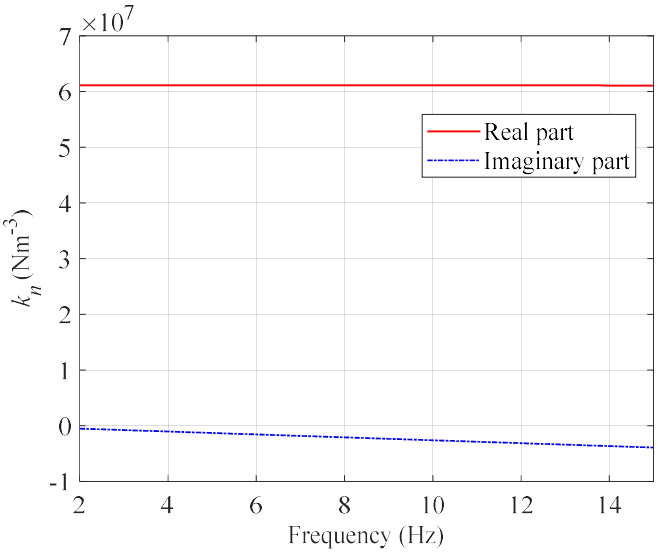

Fig. 16 Real and imaginary parts of the coefficient k_n.

As known, the dynamic characteristic of this structure can be considered as a linear system when the low excitation level (0.76Nrms) is conducted in the system. In this case, the corresponding FRF h_{32} is shown in **Fig. 17**, and the frequencies can be found in our previous work [10]. By comparing the frequency identification results of the two methods above, the absolute maximum error occurs in the fifth mode (1.62%) in Table 4. The underlying-linear FRF estimated using NSI is depicted in Fig. 14 and overlapped with the low-level experimental one. As previously stated, the correspondence is acceptable except for the fifth mode. The reason for this discrepancy is explained in [10], and it may be addressed to another form of nonlinearities not included in the present model.

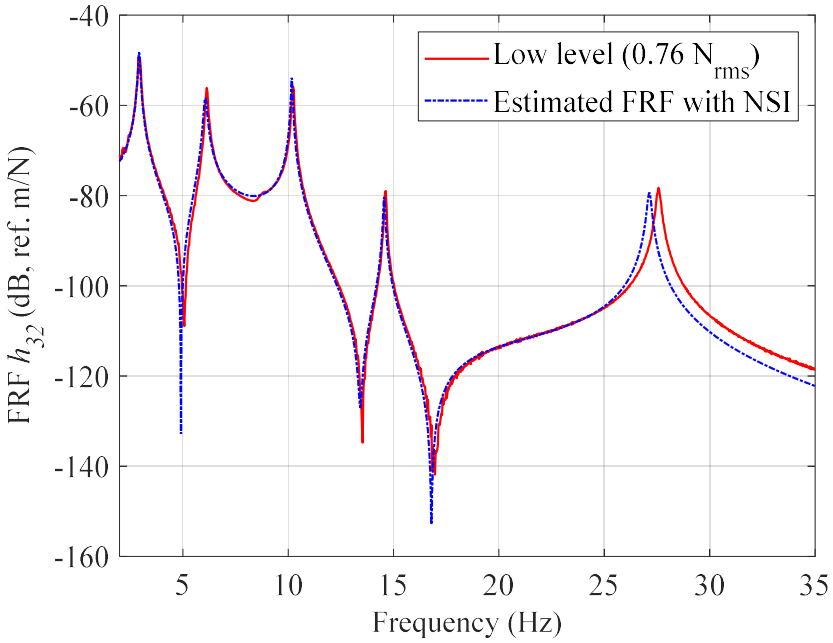

Fig. 17 Underlying linear FRF estimated using NSI and the low-level experimental one

Table 4 Comparison of frequency estimation by two methods

Mode number	1	2	3	4	5
Frequency of linear system at low-level excitation [10] (Hz)	2.94	6.13	10.23	14.61	27.58
Frequency of underlying FRF based on the proposed method (Hz)	2.95	6.07	10.18	14.55	27.14
Error/%	-0.48	0.93	0.46	0.40	1.62

Results prove the accuracy of the algorithm in identifying the frequency of the underlying linear system and also show the effectiveness of the automatic order determination, which reduces the difficulty of the identification task.

The robustness of the clustering algorithm is further investigated by assessing the effects of the threshold value δ. To this end, different values of δ are used in the clustering stage (δ=0.001,0.005,0.02,0.05,0.08). The corresponding cluster stabilization diagrams are shown in **Fig. 18**. When the threshold value (δ=0.001) is too small, it can cause some modal loss due to noise (in **Fig. 18** (a)); On the opposite side, a high value (δ=0.08) will add one more cluster with a large dispersion in **Fig. 18** (e), which can be excluded based on other tools such as underlying FRF. When the threshold is selected between 0.005 and 0.05, the results have good consistency, which verifies the robustness of the proposed method.

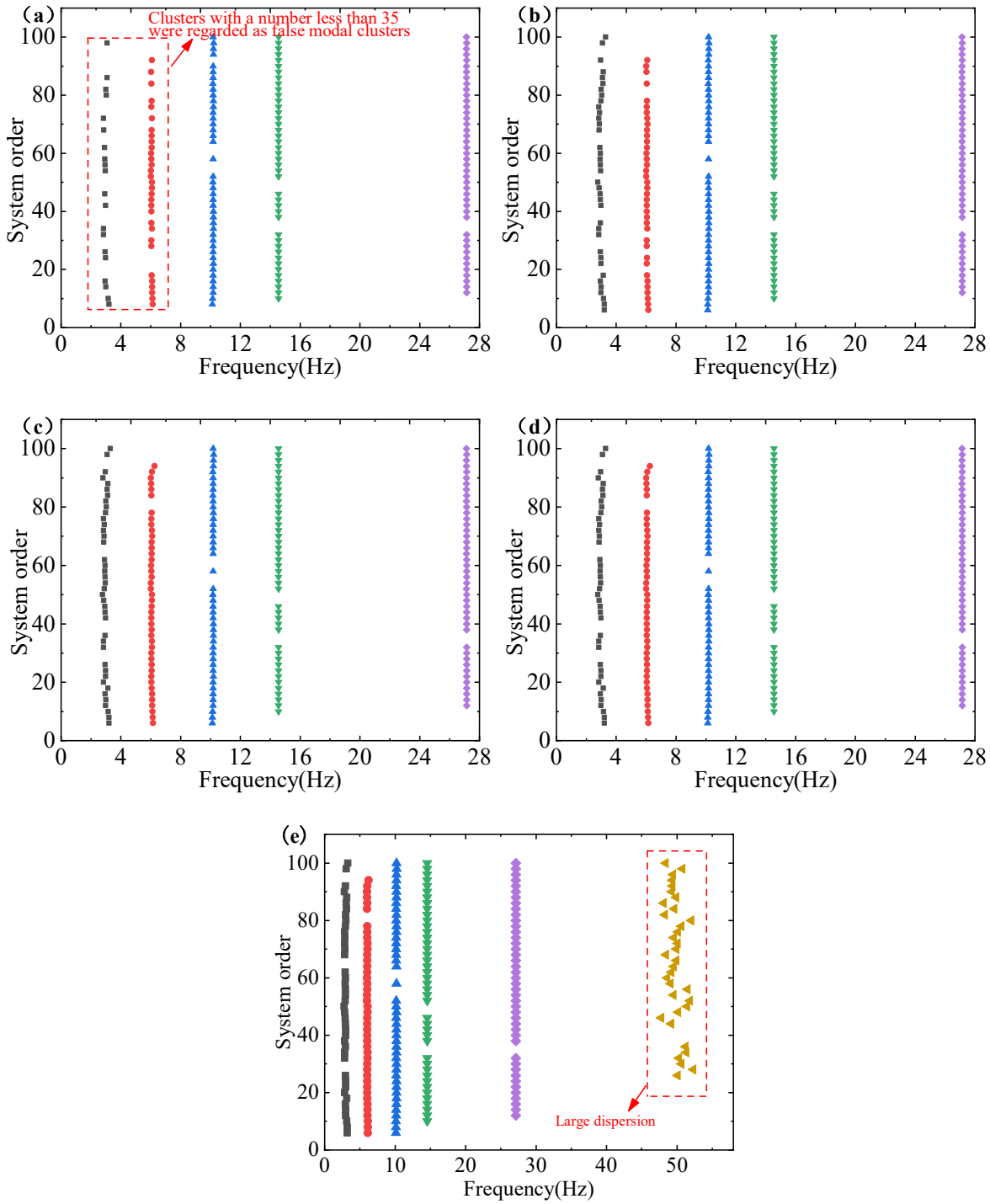

Fig. 18 The cluster stabilization diagram with the different threshold value (a) δ =0.01; (b) δ =0.005:(c) δ = 0.02; (d) δ =0.05; (e) δ = 0.08

V. Conclusion

In this paper, an automatic nonlinear system identification method is proposed based on the clustering stabilization graph and similarity filtering. The significant advantage of the method is that it can effectively eliminate the spurious modes of the underlying linear system, determine the true order of the structure, and reduce the influence of human judgment. MDOF simulation system with typical nonlinear characteristics is conducted to verify the proposed approach's effectiveness. The multilayer building with nonlinearity is investigated experimentally. Linear modal parameters can be obtained as a criterion for subsequent verification by applying low-level excitation. Further, at a high-level excitation, the method of this paper is used to determine the order of the structure and then obtain the modal parameters of the underlying linear system. By comparing with the traditional stabilization graph, the accuracy of the automatic order determination proposed is proved. Finally, nonlinear parameter coefficients are effectively identified. Under different thresholds, the method has better robustness. The above test results verify the effectiveness of the method proposed in this paper, and it has good adaptability to engineering.

Acknowledgments

This research work is supported by the National Natural Science Foundation of China (52005100, 52125209, 11602112), natural Science Foundation of Jiangsu Province (BK20190324), the Shanghai Space Science and Technology Innovation Fund (SAST2019-019), the Fundamental Research Funds for the Central Universities, the Zhishan Youth Scholar Program of SEU (2242021R41169), Natural Science Research Project of Higher Education in Jiangsu Province (20KJB460003) and the Qing Lan Project.

References

[1] Moore K J, Mojahed A, Bergman L A , et al. “Local Nonlinear Stores Induce Global Dynamical Effects in an Experimental Model Plane,” *AIAA Journal*, Vol. 57, No. 11, 2019, pp: 4953-4965. https://doi.org/10.2514/1.J058311

[2] Soize, C., Capiez-Lernout, E., and Ohayon, R., “Robust Updating of Uncertain Computational Models Using Experimental Modal Analysis,” AIAA Journal, Vol. 46, No. 11, 2008, pp. 2955–2965. https://doi.org/10.2514/1.38115

[3] Rui Zhu, Qingguo Fei, Dong Jiang, Zhifu Cao, “Dynamic Sensitivity Analysis Based on Sherman–Morrison–Woodbury Formula,” *AIAA Journal*, Vol. 57, No. 11, 2019, pp: 4992-5001.
https://doi.org/ 10.2514/1.J058280

[4] Zuo, W., and Saitou, K., “Multi-Material Topology Optimization Using Ordered SIMP Interpolation,” *Structural and Multidisciplinary Optimization*, Vol. 55, No. 2, 2017, pp. 477–491.
https://doi.org/10.1007/s00158-016-1513-3

[5] Rui Zhu, Qingguo Fei, Dong Jiang, et al. “Removing mass loading effects of multi-transducers using Sherman-Morrison-Woodbury formula in modal test,” *Aerospace Science and Technology*, 2019. Vol. 20, No. 3, 2006, pp: 505-592.
https://doi.org/10.1016/j.ast.2019.06.022

[6] Singh A, Moore K J., “Characteristic nonlinear system identification of local attachments with clearance nonlinearities,” *Nonlinear Dynamics*, Vol. 20, No. 3, 2006, pp: 505-592. 2020, 102(3):1-18.
https://doi.org/10.1007/s11071-020-06004-8

[7] Kerschen, G., et al., “Past, present and future of nonlinear system identification in structural dynamics,” *Mechanical Systems and Signal Processing*, Vol. 20, No. 3, 2006, pp: 505-592.
https://doi.org/10.1016/j.ymssp.2005.04.008

[8] Noël, J.P. and G. Kerschen, “Nonlinear system identification in structural dynamics: 10 more years of progress,” *Mechanical Systems and Signal Processing*, Vol. 93, 2017, pp: 2-35.
https://doi.org/10.1016/j.ymssp.2016.07.020

[9] Jiang, H.M, Chen J, Dong G M, Liu T, Chen G., “Study on Hankel matrix-based SVD and its application in rolling element bearing fault diagnosis,” *Mechanical Systems and Signal Processing*, Vol. 52, 2015, pp: 338-359.
https://doi.org/10.1016/j.ymssp.2014.07.019

[10] S. Vanlanduit, P. Verboven, P. Guillaume, J. Schoukens, “An automatic frequency domain modal parameter estimation algorithm,” *Journal of Sound and Vibration*, Vol. 265, No.3, 2003, pp: 647-661.
https://doi.org/10.1016/S0022-460X(02)01461-X

[11] Y. Zhang, Z. Zhang, X. Xu, H. Hua, “Modal parameter identification using response data only,” *Journal of Sound and Vibration*, Vol. 282, No.1, 2005, pp: 367-380.
https://doi.org/10.1016/j.jsv.2004.02.012

[12] F. Magalhaes, A. Cunha, E. Caetano, “Online automatic identification of the modal parameters of a long span arch bridge,” *Mechanical Systems and Signal Processing*, Vol. 23, No.2, 2009, pp: 316-329.
https://doi.org/10.1016/j.ymssp.2008.05.003

[13] Ni Zhuyu, Mu Ruinan, Xun Guangbin, Wu Zhigang, “Time-varying modal parameters identification of a spacecraft with rotating flexible appendage by recursive algorithm,” *Acta Astronautica*, Vol. 118, No.1 2016, pp: 49-53. https://doi.org/10.1016/j.actaastro.2015.10.001

[14] Bakir P G. “Automation of the stabilization diagrams for subspace based system identification,” *Expert Systems with Applications*, Vol. 38, No.12, 2011, pp: 14390-14397. https://doi.org/10.1016/j.eswa.2011.04.021

[15] Rainieri C, Fabbrocino G, “Development and validation of an automated operational modal analysis algorithm for vibration-based monitoring and tensile load estimation,” *Mechanical Systems and Signal Processing*, Vol. 60, 2015, pp: 512-534. https://doi.org/10.1016/j.ymssp.2015.01.019

[16] Marchesiello, S. and L. Garibaldi, “A time domain approach for identifying nonlinear vibrating structures by subspace methods,” *Mechanical Systems and Signal Processing*, Vol. 22, No. 1, 2008, pp: 81-101. https://doi.org/10.1016/j.ymssp.2007.04.002

[17] Marchesiello, S. and L. Garibaldi, “Identification of clearance-type nonlinearities,” *Mechanical Systems and Signal Processing*, Vol. 22, No. 5, 2008, pp: 1133-1145. https://doi.org/10.1016/j.ymssp.2007.11.004

[18] Noël, J.P. and G. Kerschen, “Frequency-domain subspace identification for nonlinear mechanical systems,” *Mechanical Systems and Signal Processing*, Vol. 40, No. 2, 2013, pp: 701-717. https://doi.org/10.1007/978-1-4614-6570-6_8

[19] Rui Zhu, Qingguo Fei, Dong Jiang, S. Marchesiello and D. Anastasio. “Identification of nonlinear stiffness and damping parameters using a hybrid approach,” *AIAA Journal*, Vol. 59, No. 11, 2021, pp: 4686-4695. https://arc.aiaa.org/doi/10.2514/1.J060461

[20] Rui Zhu, Qingguo Fei, Dong Jiang, S. Marchesiello and D. Anastasio. “Bayesian model selection in nonlinear subspace identification,” *AIAA Journal*, Vol. 60, No. 1, 2022, pp: 92-101. https://arc.aiaa.org/doi/abs/10.2514/1.J060782

[21] Noël, J.P., Marchesiello, S., and G. Kerschen, “Subspace-based identification of a nonlinear spacecraft in the time and frequency domains,” *Mechanical Systems and Signal Processing*, Vol. 43, 2014, pp: 217-236. https://doi.org/10.1016/j.ymssp.2013.10.016

[22] Marchesiello, S., A. Fasana and L. Garibaldi, “Modal contributions and effects of spurious poles in nonlinear subspace identification,” *Mechanical Systems and Signal Processing*, Vol. 74, 2016, pp: 111-132. https://doi.org/10.1016/j.ymssp.2015.05.008

[23] Xu R, Wunsch D. “Survey of clustering algorithms,” *IEEE Transactions on neural networks*, Vol. 16, No.3, 2005, pp: 645-678.
https://doi.org/10.1109/TNN.2005.845141

[24] Van Overschee P, De Moor B L. “Subspace identification for linear systems: Theory—Implementation—Applications,” *Springer Science & Business Media*, 2012.

[25] D. Anastasio, S. Marchesiello, “Free-Decay Nonlinear System Identification via Mass-Change Scheme,” *Shock and Vibration*, 2019, pp: 1-14.
https://doi.org/10.1155/2019/1759198.

[26] Gatti, Gianluca., Michael J. Brennan, and Ivana, Kovacic., “On the interaction of the responses at the resonance frequencies of a nonlinear two degrees-of-freedom system,” *Physica D: Nonlinear Phenomena*, Vol. 239, No. 10, 2010, pp: 591-599.
https://doi.org/10.1016/j.physd.2010.01.006